

RESEARCH ARTICLE

Immunomodulation and effects on microbiota after *in ovo* administration of chicken cathelicidin-2

Trynysje Cuperus¹, Marina D. Kraaij¹, Aldert L. Zomer², Albert van Dijk¹, Henk P. Haagsman^{1*}

1 Division of Molecular Host Defence, Department of Infectious Diseases & Immunology, Faculty of Veterinary Medicine, Utrecht University, Utrecht, The Netherlands, **2** Division Clinical Infectiology, Department of Infectious Diseases & Immunology, Faculty of Veterinary Medicine, Utrecht University, Utrecht, The Netherlands

* h.p.haagsman@uu.nl



OPEN ACCESS

Citation: Cuperus T, Kraaij MD, Zomer AL, van Dijk A, Haagsman HP (2018) Immunomodulation and effects on microbiota after *in ovo* administration of chicken cathelicidin-2. PLoS ONE 13(6): e0198188. <https://doi.org/10.1371/journal.pone.0198188>

Editor: Xiaonan Han, Cincinnati Children's Hospital Medical Center, UNITED STATES

Received: July 27, 2017

Accepted: May 15, 2018

Published: June 5, 2018

Copyright: © 2018 Cuperus et al. This is an open access article distributed under the terms of the [Creative Commons Attribution License](https://creativecommons.org/licenses/by/4.0/), which permits unrestricted use, distribution, and reproduction in any medium, provided the original author and source are credited.

Data Availability Statement: The microbiome meta data can be found in the European Nucleotide Archive. The ENA Study accession number is: PRJEB19392. The secondary study accession number is: ERP021418.

Funding: The work was supported by the Immuno Valley ALternatives to ANTibiotics (ALTANT) Animal Specific Immunomodulatory Antimicrobials (ASIA) program of the Dutch Ministry of Economic Affairs. This program is a public-private partnership. The funders had no role in the study

Abstract

Host Defense Peptides (HDPs) such as cathelicidins are multifunctional effectors of the innate immune system with both antimicrobial and pleiotropic immunomodulatory functions. Chicken cathelicidin-2 (CATH-2) has multiple immunomodulatory effects *in vitro* and the D-amino acid analog of this peptide has been shown to partially protect young chicks from a bacterial infection. However, the mechanisms responsible for CATH-2 mediated *in vivo* protection have not been investigated so far. In this study, D-CATH-2 was administered *in ovo* and the immune status and microbiota of the chicks were investigated at 7 days posthatch to elucidate the *in vivo* mechanisms of the peptide. In three consecutive studies, no effects on numbers and functions of immune cells were found and only small changes were seen in gene expression of Peripheral Blood Mononuclear Cells (PBMCs). In two studies, intestinal microbiota composition was determined which was highly variable, suggesting that it was strongly influenced by environmental factors. In both studies, *in ovo* D-CATH-2 treatment caused significant reduction of Ruminococcaceae and *Butyricoccus* in the cecum and *Escherichia/Shigella* in both ileum and cecum. In conclusion, this study shows that, in the absence of an infectious stimulus, *in ovo* administration of a CATH-2 analog alters the microbiota composition but does not affect the chicks' immune system posthatch.

Introduction

Host Defense Peptides (HDPs) such as cathelicidins and defensins are important effector molecules of the innate immune system. These peptides are multifunctional as they show both broad-spectrum antimicrobial activity but also have many immunomodulatory functions [1,2]. In the search for alternatives to antibiotics, HDPs are considered promising candidates for both human and veterinary applications [3,4]. Initially the antimicrobial activity of HDPs was seen as their most important asset in their development as anti-infective drugs. However, antimicrobial activity of many HDPs is severely inhibited by components present in

design, data collection and analysis, decision to publish, or preparation of the manuscript.

Competing interests: The authors have declared that no competing interests exist.

physiological environments such as salt or proteins [5–7]. Therefore, immunomodulatory activities are now believed to be essential for *in vivo* protection by these peptides and HDP analogs without antibacterial activity have been shown to provide protection against infections in animal models [8,9]. Chicken cathelicidin-2 (CATH-2) is one of the four cathelicidins of the chicken. Previously, a D-amino acid analog of this peptide (D-CATH-2) was described to protect young chickens against an *Escherichia coli* infection after administration into embryonated eggs (*in ovo*), a technique used commercially to administer vaccines to broiler eggs [10]. Immunomodulation is believed to be the mechanism behind this protection as direct antimicrobial activity is improbable due to the small amount of D-CATH-2 administered and the time gap of 10 days between peptide administration and onset of infection. Immunomodulatory activities of CATH-2 have been shown *in vitro*, including induction of chemokine production, inhibition of LPS-induced inflammatory mediators and enhancement of DNA-induced macrophage activation [11,12]. Similar to CATH-2, most immunomodulatory activities described for HDPs are identified by *in vitro* research. Therefore, the question remains which immunomodulatory mechanisms drive the anti-infective *in vivo* effects of CATH-2 and HDPs in general. In this study, we analyzed the immunomodulatory effect of *in ovo* administered D-CATH-2 by investigating the immune status of 7 day old chicks. This timepoint was chosen to correspond with our previous experiment in which we challenged chicks with *E. coli* at 7 days of age after *in ovo* administration with D-CATH-2 [10]. We investigated the number of immune cells in peripheral blood and organs and assessed the functionality of PBMCs and dendritic cells (DC). In addition, the effects of *in ovo* D-CATH-2 on the intestinal morphology and microbiota were determined.

Materials and methods

Synthesis of cathelicidin peptides

D-CATH-2 (all D-amino acid sequence: RFGRFLRKIRRFKPKVTITIQGSARF-NH₂) was generated by solid-phase synthesis using Fmoc-chemistry and purified to >95% by RP-HPLC by CPC Scientific Inc. (Sunnyvale, USA).

Animals

This study was conducted in accordance with the Dutch Experiments on Animals Act and conformed the European standards (European Directive 2010/63/EU). All separate animal experiments were approved by the Central Authority for Scientific Procedures on Animals (CCD) (Permit number: 2014.II.05.37). Ross 308 broiler eggs at day 18 of embryonic development (ed18) were obtained from a commercial hatchery (Lagerwey, Lunteren, The Netherlands). Chickens were housed in negative pressure HEPA isolators where temperature was gradually decreased from 35 °C to 27.5 °C over 7 days posthatch and fed a commercial broiler diet ad libitum (Research Diet Services, Wijk bij Duurstede, The Netherlands, no antibiotics or coccidiostats added).

In vivo experiments

Peptide preparation and injection was similar to Cuperus *et al.* [10]. Briefly, D-CATH-2 was dissolved in PBS (1.48 mM NaH₂PO₄·H₂O, 8.06 mM Na₂HPO₄, 20 mM NaCl, pH 7.27, filter sterilized) to a concentration of 0.22 mg/ml, to which cholesterol (5% v/v, 2 mg/ml in absolute ethanol) was added. Three days before hatch (ed18, estimated embryo weight = 22 g), 1 mg/kg D-CATH-2 or buffer was administered *in ovo* into the amniotic cavity using a 1 inch, 21G needle injected up to the hilt. Posthatch, only male chickens were selected (n = 6–8/group) and

housed in separate isolators per experimental treatment. Animals were euthanized by electrocution followed by cardiac puncture and organs, blood and intestinal content were collected. Three separate *in vivo* experiments were conducted in which the same batch of chicken feed was used.

PBMC isolation and tissue single cell isolation

Peripheral blood mononuclear cells (PBMCs) were isolated from whole blood using a Ficoll gradient. Spleen and cecal tonsil single cell suspensions were made by gently pressing the tissue through a 70 μ M cell strainer followed by a Ficoll gradient for spleen samples. Cells were frozen at -80 °C until further analysis.

Whole blood and tissue flow cytometry

Whole blood samples were incubated with the following labelled antibodies: CD45-APC (clone LT40, dilution 1:200), CD3-PE (clone CT-3, dilution 1:200), KUL01-FITC (dilution 1:50, Southern Biotech, Birmingham, AL, USA) and unlabeled antibodies: Bu-1 (clone AV20, dilution 1:500), MHC-II (clone 2G11, dilution 1:500) (Southern Biotech), CD41/CD61 (clone 11C3, dilution 1:100) and CD40 (clone AV79, dilution 1:100) (AbD Serotec, Kidlington, UK) for 30 min at 4 °C. After washing, samples with unlabeled antibodies were subsequently incubated for 30 min with secondary BV421 or PerCP-Cy5.5-labelled rat-anti-mouse antibodies (clone RMG1-1, dilution 1:500/1:800 respectively, BioLegend, San Diego, CA, USA). Samples were washed and analyzed by flow cytometry (FACSCantoII, BD Biosciences, San Jose, CA, USA) using FlowJo analysis software. Absolute cell numbers were determined using BD Tru-count absolute counting tubes (BD Biosciences) according to the manufacturer's protocol. Cell suspensions from cecal tonsils and spleen were also stained with above-mentioned antibodies and protocol.

Phagocytosis assay

PBMCs were defrosted and seeded in duplicate in black 96-well plates (5×10^6 cells/well) in RPMI-1640 medium without Phenol Red. After 1 hour of incubation at 41 °C, medium was replaced with pHrodo Green *E. coli* bioparticles (ThermoFisher, Waltham, MA, USA) suspended in RPMI-1640 without Phenol Red. Fluorescence (488/520 nm) was measured for up to 6 hours in a microplate reader at 41 °C.

Oxidative burst assay

PBMCs were defrosted and seeded in black 96-well plates (1.5×10^6 cells/well) in RPMI-1640 without Phenol Red containing 10% FCS (Bodinco, Alkmaar, The Netherlands) and 1% penicillin/streptomycin (Life Technologies, Paisley, UK). After overnight incubation at 41 °C, medium was replaced with RPMI-1640 containing the profluorescent probe 2',7'-dichloro-fluorescein-diacetate (DCFH-DA, 10 μ g/ml, Sigma-Aldrich, Zwijndrecht, The Netherlands). Fluorescence (488/520 nm) was measured in a microplate reader at 41 °C for up to 3 hours.

Mixed lymphocyte reaction

In an allogeneic mixed lymphocyte reaction (MLR), responder PBMCs (from healthy adult chickens) were labelled with 5 μ M CFSE (carboxyfluorescein succinimidyl ester, BioLegend, San Diego, CA, USA) in PBS for 10 min at 37 °C. To quench the staining, RPMI-1640 medium containing 10% FCS was added. In a 96-wells plate, 1×10^5 labelled responder cells were added to the PBMCs from the experimental chickens in ratios ranging from 8:1–1:64. In other

experiments, 1×10^5 responder PBMCs were added to bone marrow-derived dendritic cells from experimental chickens in ratios ranging from 2:1–1:64. Cell mixtures were incubated for 5 days at 41 °C and analyzed by flow cytometry using FlowJo analysis software. The percentage of proliferation was calculated relative to the proliferation in responder cells alone.

PBMC microarray

RNA ($n = 6/\text{group}$) was isolated from PBMCs using Trizol (Ambion, Paisley, UK) precipitation and purified using RNeasy columns (Qiagen, Venlo, The Netherlands). An automated system (Caliper Life Sciences, Hopkinton, MA, USA) was used to perform cDNA synthesis, labeling, quantification, quality control by Bioanalyzer and fragmentation, starting with 3 μg total RNA from each samples as previously described [13]. Per treatment, three samples were labeled with Cy5 and co-hybridized with reference RNA (pooled RNA from all experimental samples) labeled with Cy3. The remaining samples were labeled and hybridized the opposite way (Cy3-labeled RNA from experimental samples with Cy5-labeled reference RNA). Microarrays used were chicken whole genome gene expression arrays V2 (Agilent, Santa Clara, CA, USA) representing 42034 *Gallus gallus* 60-mer probes in a 4x44K layout. Probe sequences were re-annotated by BLAST searching against the chicken genome version 76.4 at ENSEMBL. Microarray hybridization and washing was performed with a HS4800PRO system with Quad-Chambers (Tecan, Männedorf, Switzerland) using 1000 ng, 1–2% Cy5/Cy3 labeled cRNA per channel. Slides were scanned on an Agilent G2565BA scanner. Data was extracted using ImageGene 8.0 (BioDiscovery, Hawthorne, CA, USA) and Loess normalization was performed on mean spot intensities [14]. Gene-specific dye bias was corrected by a within-set estimate [15]. Differences in gene expression between treatment groups were analyzed by Linear Model for Microarray Analysis (LIMMA) with Benjamini-Hochberg FDR correction. Genes with $p < 0.05$ and fold-change > 2 were considered significantly changed. Because the Bioanalyzer results showed monospecific peaks in the cRNA pointing to contamination of the RNA, principal component analysis (PCA) was performed on \log_2 transformed expression values of genes with a > 2 -fold difference between samples. The principal component (PC2) with the highest correlation to the peaks from the Bioanalyzer results was then used as a covariate in LIMMA representing severity of contamination. Results of the corrected and uncorrected LIMMA analyses were compared to obtain significantly changed genes.

Dendritic cell culture

Bone marrow was harvested from the chicken's femurs and tibias and homogenized through a 70 μm cell strainer. Cells were centrifuged and resuspended in RPMI-1640 medium containing 5% chicken serum, 1% GlutaMAX-I and 0.5% penicillin/streptomycin (Life Technologies). Bone marrow cells were seeded at a concentration of 2.5×10^6 cells/ml in 6-well plates and optimally diluted concentrations of recombinant chicken IL-4 and GM-CSF were added [16]. Plasmids were kindly provided by Prof. P. Kaiser and L. Rothwell (The Roslin Institute, Edinburgh, UK). Cells were cultured for 7 days at 41 °C, at days 3 and 5, medium was replaced with fresh medium containing IL-4 and GM-CSF. After harvesting at day 7, cells were stained with MHC-II, CD40 and CD86 (AbD Serotec, Kidlington, UK) antibodies and secondary BV421-labelled anti-mouse antibody as described above. Cells were washed and analyzed by flow cytometry and FlowJo analysis software.

Villus/crypt ratio and goblet cell measurements

Tissue samples of duodenum, jejunum and ileum were fixed in 4% formaldehyde and paraffin-embedded. Tissue sections of 2 μm were stained with the combined Alcian Blue (pH 2.5)/

PAS procedure according to Luna *et al* [17]. Microscopic images of representative cross-sections were analyzed using cellSens Dimension (Olympus, Tokyo, Japan) software. Per intestinal segment 5 representative and completely paired villus-crypt units were measured. The villus/crypt ratio was determined as the length of the villi divided by the depth of the mucosal crypt region. Size and density of Alcian Blue/PAS positive goblet cells was determined in 5 representative well oriented villi per intestinal sample.

Microbiota analysis

Bacterial DNA was extracted from embryonic (ed18) intestinal samples (intestinal tissue including contents, harvested under sterile circumstances) and jejunal and cecal contents of 7 days old chicks using a phenol/bead-beating and magnetic bead separation method as described previously [18]. Per sample, 1 ng of DNA was amplified using F515/R806 primers (Caporaso *et al*, 2011) based on the V4 hypervariable region of the 16S rDNA gene (details of amplicon PCR described in Kozich *et al*, 2013). After amplification, samples were sequenced by Illumina MiSeq (Illumina Inc., San Diego, CA, USA) and processed using modules implemented in Mothur V1.31.2 [19]. Reads were trimmed using Btrim (Kong, 2011) with a sliding window size of 5 nt and an average quality score of 25 and contigs between read pairs were assembled. The sequences were aligned to the reference alignment SILVA SEED (release 102, www.mothur.org/wiki/Silva_reference_files). The ends of the sequences were trimmed in order that the sequences all started and ended at the same alignment coordinates. The resulting sequences were screened for chimeras using UCHIME (Edgar *et al*, 2011). Sequence data was subsampled to the lowest number of reads and sequences observed less than 10 times were removed. High quality aligned sequences were taxonomically classified using the Ribosomal Database Project-II naïve Bayesian classifier [20], requiring a 60% pseudobootstrap confidence score. Aligned sequences were subsequently clustered into operational taxonomic units (OTUs, defined by 97% similarity) using the average linkage clustering method.

PCA was performed on log transformed OTU abundances of all OTUs accounting for at least 1% of the reads in one sample. The relative abundance of OTUs and higher taxonomic levels were compared between treatment groups and statistically tested using the Mann-Whitney *U* test. The Benjamini-Hochberg FDR procedure was used for multiple testing correction.

Statistics

Statistical analysis was performed using SPSS 22 software (IBM, Armonk, USA). In separate *in vivo* experiments, differences between treatment groups were tested using unpaired *t*-tests and Mann-Whitney *U* tests for non-normally distributed data. In addition, overall differences in variables measured in all three experiments (weight, whole blood leukocyte populations, phagocytosis, oxidative burst, VC ratio, goblet cell parameters) were analyzed using a General Linear Model. Differences were considered statistically significant if $p < 0.05$.

Results

Chicken bodyweight

To investigate a possible effect of *in ovo* administration of a CATH-2 analog on chicken growth, animals were weighed at multiple timepoints posthatch. Bodyweight was not different between non-treated and D-CATH-2 treated animals (S1 Fig) at any timepoint.

Leukocyte numbers in peripheral blood, spleen and cecal tonsils

Leukocyte numbers were measured in peripheral blood to investigate a possible effect of *in ovo* administration of D-CATH-2 on the systemic immune status of the chickens. In addition to total leukocytes (CD45), populations of mononuclear phagocytes (KUL01), T-cells (CD3), B-cells (Bu-1) and thrombocytes (CD41/CD61) were determined (Fig 1). In Exp I, a trend towards an increase of KUL01 positive cells was seen in D-CATH-2 treated animals, both in percentage in whole blood (Fig 1c, $p = 0.071$) and in absolute cell numbers (Fig 1d, $p = 0.068$). However, in the two following experiments, differences in KUL01 positive cells were not observed. In the other measured leukocyte populations, no differences were seen in any of the experiments between control and peptide treated animals (Fig 1a, 1b, 1e–1h). In addition, expression of MHC-II and CD40, two cell surface proteins involved in antigen presentation, was measured on the KUL01 positive population in samples derived from Exp II. Expression of these markers was not different between control and D-CATH-2 treated animals (S2 Fig).

In samples of Exp II, leukocyte populations were also determined in spleen and cecal tonsils. None of the determined populations showed significant differences between control and D-CATH-2 treated animals (S3 Fig).

Functional capacity of PBMCs

To examine whether *in ovo* administration of D-CATH-2 could have an effect on PBMC function we analyzed phagocytosis and oxidative burst in samples from all three experiments and proliferative capacity in samples from Exp I. An increased capacity for phagocytosis was seen in PBMCs from D-CATH-2 treated animals in samples from Exp I ($p = 0.002$), while in the other two experiments no differences in phagocytosis were observed between treatment groups (Fig 2a). A similar response was found for oxidative burst; in PBMCs of Exp I a trend towards increased oxidative burst ($p = 0.053$) was seen in samples from D-CATH-2 treated chickens (Fig 2b). Samples from Exp II or III or overall results showed no difference. Stimulation of the oxidative burst by phorbol myristate acetate (PMA, 1 $\mu\text{g/ml}$) yielded similar results (S4 Fig). In addition, a mixed lymphocyte reaction (MLR) was performed to measure the capacity of PBMCs from the experimental chickens to activate T cells. The proliferation measured was similar in samples from D-CATH-2 treated chickens compared to control chickens (Fig 2c). These data indicate *in ovo* treatment with D-CATH-2 does not affect the functional capacity of PBMCs at 7 days posthatch.

PBMC microarray

To analyze differences in gene expression in PBMCs from control and D-CATH-2 treated chickens, a whole genome microarray was performed on samples from Exp III. We observed 56 differentially expressed genes with a fold-change of more than 2. However, contamination of the RNA was observed, potentially caused by excessive amounts of globin mRNA (originating from red blood cells). PCA on gene expression differences revealed that 28 of the differentially expressed genes correlated with the observed RNA contamination with an $R^2 > 0.5$, indicating that measured expression of these genes could be strongly influenced by the (globin) contamination. Interestingly, 85% (24/28) of these genes were downregulated in PBMCs from D-CATH-2 treated animals compared to the control treatment. The differentially expressed genes for which a gene description was available are shown in S1 Table.

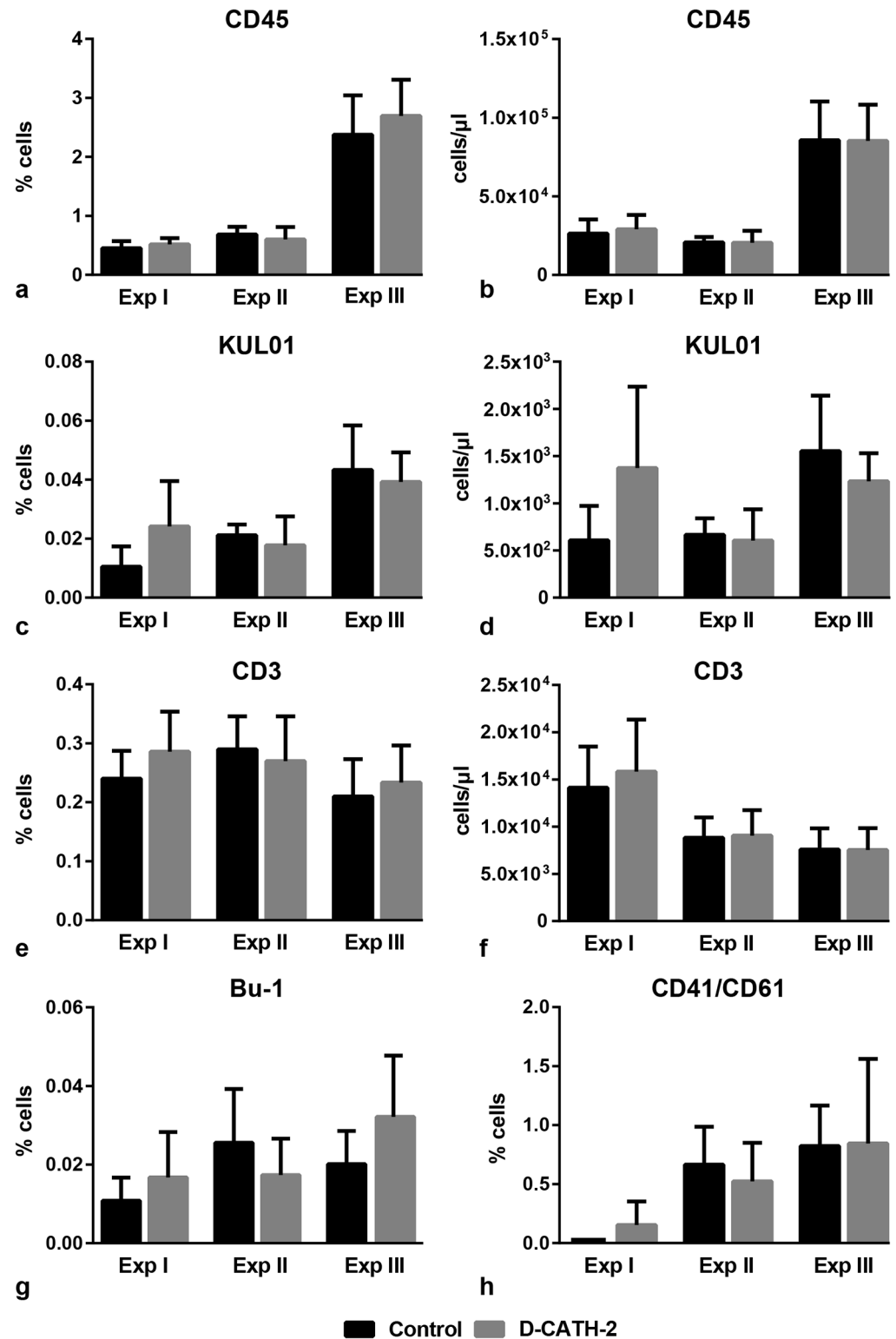


Fig 1. Leukocyte populations in peripheral blood. Data from three repeated experiments. (a)-(b) total leukocytes (CD45), (c)-(d) mononuclear phagocytes (KUL01), (e)-(f) T-cells (CD3), (g) B-cells (Bu-1), (h) thrombocytes (CD41/CD6). Depicted are mean percentages of total cells (a,c,e,g,h) or mean absolute cell numbers (b,d,f) \pm s.d., n = 6-8/group. Data of independent experiments were analyzed by an unpaired *t*-test, while combined data were analyzed using a General Linear Model.

<https://doi.org/10.1371/journal.pone.0198188.g001>

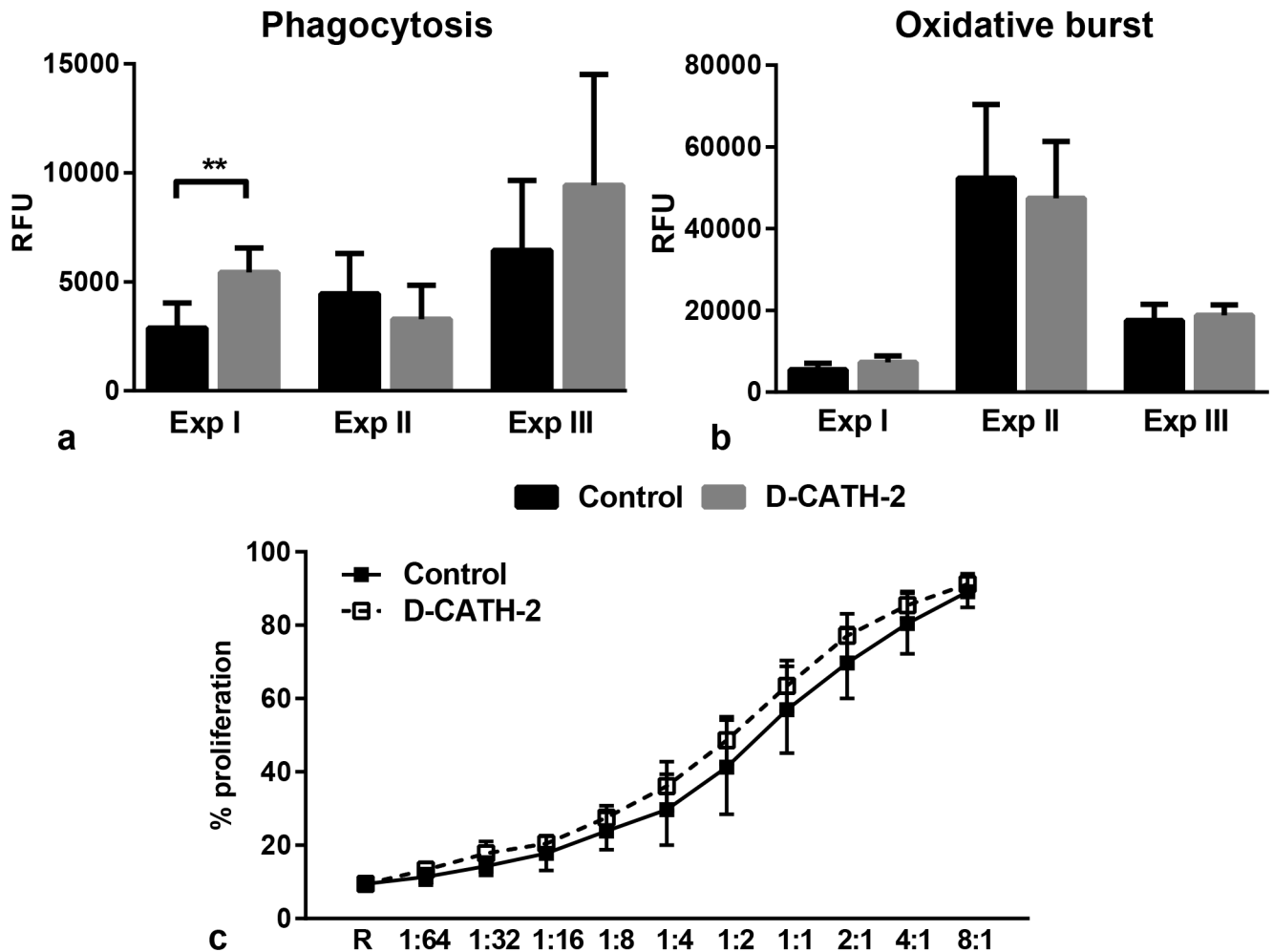


Fig 2. PBMC functions measured by *ex vivo* assays. (a) Phagocytosis measured by uptake of pHrodo Green labelled *E. coli*. Increase in fluorescence from 1–6 hours of incubation. Data from three repeated experiments, (b) Oxidative burst measured by conversion of DCFH-DA to fluorescent DCF. Increase in fluorescence in 3 hours of incubation. Data from three repeated experiments, (c) Proliferation of responder PBMCs measured by MLR, Samples from Exp I, R = responder cells alone. Depicted are mean \pm s.d., n = 5–8/group, ** = $p < 0.01$. Data from independent experiments were analyzed by an unpaired *t*-test, combined phagocytosis and oxidative burst data were analyzed by a General Linear Model.

<https://doi.org/10.1371/journal.pone.0198188.g002>

Phenotype and function of bone-marrow derived dendritic cells

In addition to PBMCs, bone-marrow derived dendritic cells from samples of Exp I were analyzed to determine the effect of *in ovo* administration of D-CATH-2 on this cell type. After 7 days of differentiation, DC phenotype was not different between cells derived from control chickens or chickens treated with D-CATH-2 (Fig 3a). In addition, expression of cell surface markers MHC-II, CD40 and CD86 was similar in cells from both treatment groups (Fig 3b). In an MLR of DCs with responder PBMCs, no difference was observed between the proliferative capacity of DCs from control chickens or from chickens treated with D-CATH-2 (Fig 3c).

Intestinal architecture and goblet cell parameters

The ratio of villus height to crypt depth (VC ratio) was measured to determine the effect of *in ovo* administration of D-CATH-2 on intestinal development. In the duodenum, VC ratio was not different between intestinal samples from control or treated chickens in any of the three

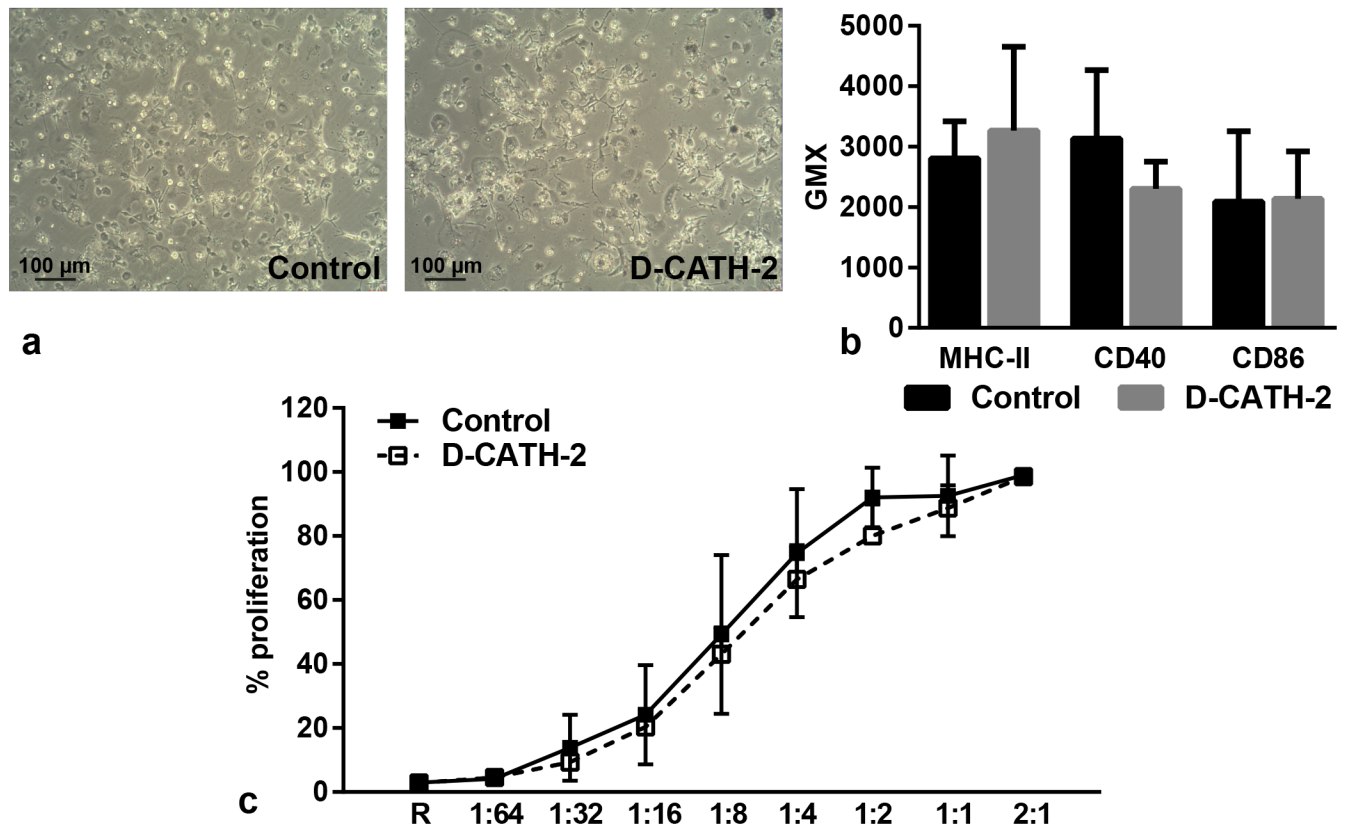


Fig 3. Phenotype and function of dendritic cells derived from Exp I. (a) Representative phenotype of bone-marrow derived DCs after 7 days of differentiation with IL-4 and GM-CSF (magnification: 100x), (b) MHC-II, CD40 and CD86 expression measured at day 7, (c) Proliferation of responder PBMcs measured by MLR, R = responder cells alone. Depicted are mean \pm s.d., n = 5-6/group. Data were analyzed by an unpaired *t*-test.

<https://doi.org/10.1371/journal.pone.0198188.g003>

experiments (Fig 4a). In addition, numbers and size of goblet cells were determined as a measure of intestinal mucus production. Goblet cell numbers were not affected by D-CATH-2 in the duodenum in any of the experiments (Fig 4b). Goblet cell size in the duodenum was increased in D-CATH-2 treated animals in Exp I ($p = 0.037$, Fig 4c) and also significantly increased when the data from three experiments were combined ($p = 0.036$, Fig 4d). VC ratio or goblet cell parameters were not different between treatment groups in the ileum or jejunum (S5 Fig).

Microbiota

Microbiota composition in the ileum and cecum was determined in samples from Exp I and III (Fig 5a and 5b). In addition, DNA from embryonic intestinal samples (ed18) was analyzed to determine the possible presence and composition of microbiota at the time of *in ovo* injection. However, bacterial DNA concentrations in the embryonic intestines were extremely low and far below the minimal input for sequencing, indicating no measurable microbiota was present in these samples. The global differences in bacterial composition of the treatment groups were analyzed by performing principal component analysis (PCA) on OTU abundances. In the analysis of the separate experiments, a clear separation could be seen between samples of the different treatment groups (cecum: Fig 5c and 5d, ileum: Panels a and b in S6 Fig). However, when data from the two experiments were combined, samples from control or D-CATH-2 treated groups did not cluster, instead all four analyzed groups clustered

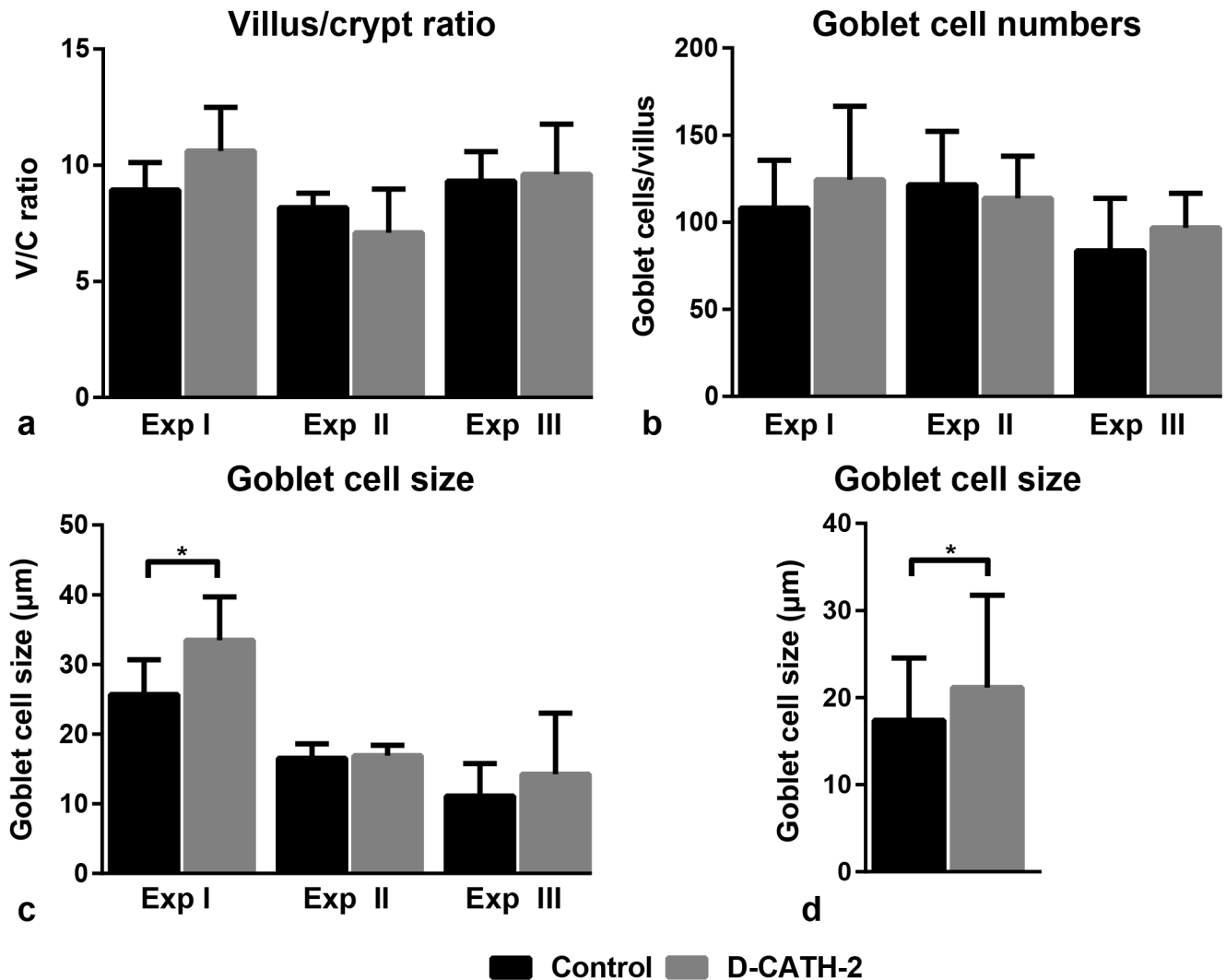


Fig 4. Intestinal architecture and goblet cell parameters in duodenum of 7 day old chicks. Data from three repeated experiments. (a) Villus/crypt ratio, (b) Goblet cell numbers per villus, (c) Goblet cell size, (d) Goblet cell size, combined data from three repeated experiments. Depicted are mean \pm s.d., $n = 6-7/\text{group}$, * = $p < 0.05$. Data were analyzed by an unpaired *t*-test, combined data were analyzed using a General Linear Model.

<https://doi.org/10.1371/journal.pone.0198188.g004>

separately, most strongly in the cecum (Fig 5e, Panel c in S6 Fig). These results indicate that the composition of the microbiota is not only affected by treatment, but also by other influences such as environment considering that the treatment groups were housed separately.

The influence of group environment was also apparent in observed differences in relative bacterial abundance. Between control and CATH-2 treatment groups, in both Exp I and III many significant differences were observed; however, these were experiment specific. Only a small number of bacterial families and genera were affected by D-CATH-2 treatment in both studies (Fig 6).

In the ileum, the abundance of the family of Streptococcaceae (Lactobacillales) was different between treatments in both experiments, but the results showed contrasting directions in Exp I ($p = 0.004$) and Exp III ($p = 0.011$) (Fig 6a). At the genus level, *Escherichia/Shigella* (Enterobacteriaceae) was reduced by D-CATH-2 treatment in both experiments ($p = 0.029$ and 0.022 respectively, Fig 6b). *Lactococcus* abundance was decreased by D-CATH-2 in both experiments

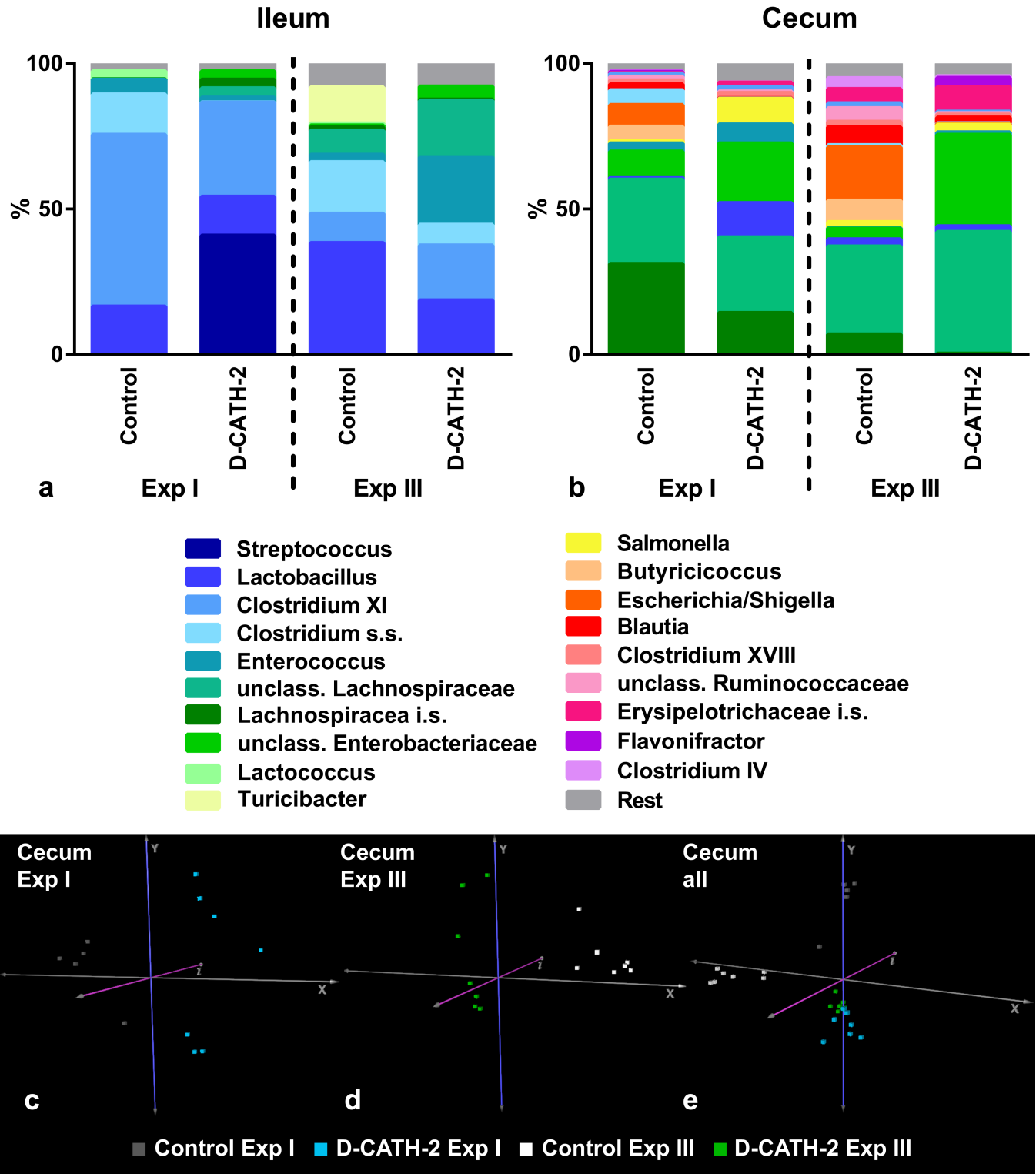


Fig 5. Microbiota at 7 days of age. Major bacterial genera in the chicken ileal (a) and cecal (b) content (n = 5-8/group). Depicted are the genera present at >1% average relative abundance across all treatment groups in their respective location. PCA plots of the bacterial communities in individual samples. (c) cecal microbiota in Exp I, (d) cecal microbiota in Exp II, (e) combined cecal microbiota data from Exp I and III.

<https://doi.org/10.1371/journal.pone.0198188.g005>

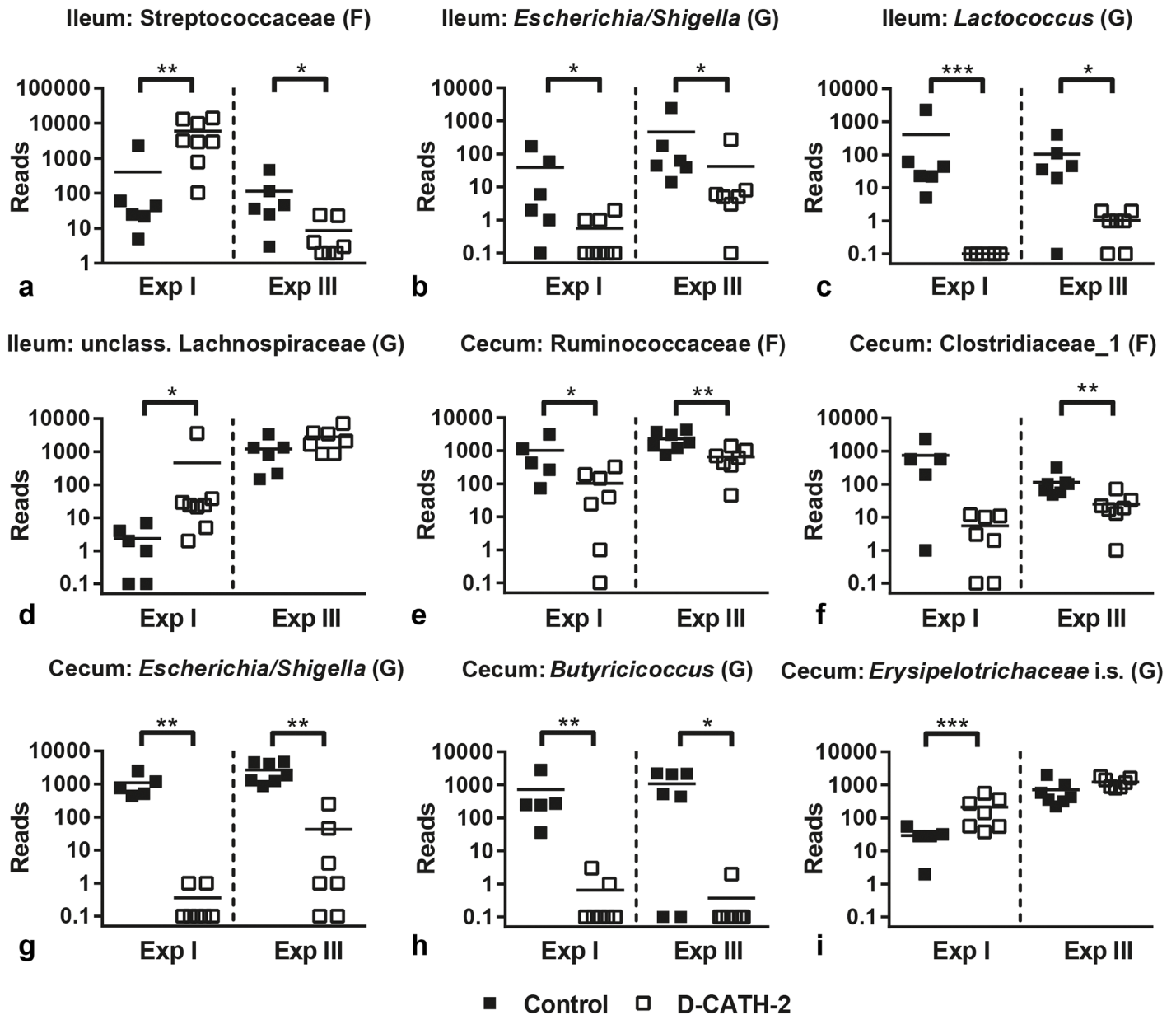


Fig 6. Relative bacterial abundance in selected families (F) and genera (G). Ileum: (a) Streptococcaceae, (b) *Escherichia/Shigella*, (c) *Lactococcus*, (d) unclassified Lachnospiraceae. Cecum: (e) Ruminococcaceae, (f) Clostridiaceae_1, (g) *Escherichia/Shigella*, (h) *Butyricoccus*, (i) *Erysipelotrichaceae* incertae sedis. Reads were normalized to total number of reads per sample. * = $p < 0.05$, ** = $p < 0.01$, *** = $p < 0.001$. Data were analyzed using the Mann-Whitney *U* test.

<https://doi.org/10.1371/journal.pone.0198188.g006>

($p = 0.0006$ and 0.013 respectively, Fig 6c). The abundance of unclassified Lachnospiraceae was increased in the ileum in Exp I ($p = 0.007$) and showed a trend towards increase in Exp III ($p = 0.063$, Fig 6d).

In the cecum, two families of Clostridiales; Ruminococcaceae ($p = 0.028$ for Exp I and $p = 0.006$ for Exp II) and Clostridiaceae_1 ($p = 0.060$ for Exp I and $p = 0.006$ for Exp II) were affected by D-CATH-2 treatment in both experiments (Fig 6e and 6f), though reduction of Clostridiaceae_1 in Exp I was not significant. At the Genus level, similar to ileum, *Escherichia/Shigella* (Enterobacteriaceae) was reduced ($p = 0.002$ and 0.002 respectively, Fig 6g).

D-CATH-2 reduced *Butyrivibrio* (Ruminococcaceae) in both experiments ($p = 0.002$ and 0.020 respectively, Fig 6h). Finally, *Erysipelotrichaceae* incertae sedis in the cecum was increased in D-CATH-2 treated animals in Exp I ($p = 0.009$) and showed a trend towards increase ($p = 0.064$) in Exp III as well (Fig 6i).

Alpha diversity was not reproducibly different between treatment groups in either cecum or ileum (S7 Fig). In Exp I, differences in OTU numbers were not seen between control and D-CATH-2 treated chickens, while in Exp III OTU numbers were significantly lower in the cecum of D-CATH-2 treated animals compared to control animals (Panel a of S7 Fig). Similar differences between experiments were obtained with a Shannon diversity analysis (Panel b of S7 Fig).

Discussion

The study described here aimed to elucidate the mechanisms behind the protection of young chicks against colibacillosis after *in ovo* administration of the HDP analog D-CATH-2 which we described in a previous article [10]. Multiple parameters reflecting immune status were measured and in addition, the influence of CATH-2 *in ovo* administration on intestinal morphology and microbiota was analyzed.

Evidence of *in vivo* immunomodulatory effects of HDPs was previously shown in mouse models. Firstly, IDR-1, an HDP analog with no *in vitro* antimicrobial activity was reported to protect mice from infections with multiple bacterial pathogens through effects on monocytes and macrophages [9]. HDP administration was also shown to protect against endotoxic shock by decreasing LPS-induced inflammatory mediators [21,22]. In our study, *in ovo* D-CATH-2 administration did not reproducibly affect the measured immune parameters, including leukocyte numbers in blood and organs and functionality of PBMCs and DCs. In addition, gene expression of PBMCs showed only very limited changes in our study. The main difference between the studies mentioned and our set of experiments is the presence or absence of an infectious stimulus. Whereas in our previous *in vivo* study with D-CATH-2 in infected animals changes in leukocyte numbers were apparent [10], the present study focused on the effect of CATH-2 administration on the immune system in unstimulated animals, which might explain the lack of observed effects. Similarly, uninfected mice treated intratracheally with LL-37 or IDR-1 showed no changes in lung cytokine responses [23] and uninfected CRAMP knockout mice have similar blood and lung leukocyte numbers as wildtype mice [24,25]. Moreover, in two studies in which bacterially derived cationic peptides were fed to chickens, effects on *ex vivo* leukocyte functions were only seen if an additional stimulus such as PMA or CpG was present [26,27]. However, in the present study we saw no change in PBMC oxidative burst even when stimulated by PMA. Finally, although all chickens used in our experiments appeared healthy, presence of an undetected infectious stimulus could have led to the effects on KUL01 cell numbers and phagocytosis in Exp I, while these effects were absent in Exp II and III. A possible mechanism explaining differences in CATH-2 effects between naïve and stimulated animals could be so-called trained immunity. This process was previously shown for several stimuli such as whole *C. albicans* or β -glucan and works through epigenetic reprogramming of cells [28,29]. To successfully decipher *in vivo* immunomodulatory mechanisms of CATH-2 in the future, studies comparing naïve and stimulated animals are needed and additionally epigenetic analyses should be performed. Independent of the mechanism, the absence of an immune response in naïve treated animals is positive for drug development as it indicates this peptide has no pro-inflammatory side effects.

The villus/crypt ratio of the intestine is a measure for intestinal functionality and development and measurements of goblet cell size and numbers may give information about intestinal

mucus production. These parameters undergo drastic changes in the developing chick, both pre- and posthatch [30–32]. The parameters can be negatively affected by infections of intestinal pathogens such as *Salmonella*, while several feed additives like butyrate and mannanoligosaccharide are able to positively influence intestinal morphology [33–36]. Villus/crypt ratio and goblet cell numbers were not affected by *in ovo* administration of D-CATH-2, showing that *in ovo* administration of this CATH-2 analog has no deleterious effect on intestinal development. In addition, a small increase of goblet cell size in the duodenum in response to D-CATH-2 administration was seen, which could indicate D-CATH-2 might increase mucus production. LL-37 has previously shown to increase mucus production *in vitro* [37]. Similar to the immunomodulatory effects, *in ovo* administration of D-CATH-2 might show more effect on these parameters in the presence of an infectious stimulus. Further studies should be conducted to investigate whether CATH-2 analogs could protect against pathogen-induced intestinal damage as was recently shown for administration of a cathelicidin analog in piglets with post-weaning diarrhea [38].

The intestinal microbiota is strongly linked to host immunity, both influencing and being influenced by the immune system [39–41]. Since in our studies D-CATH-2 was administered during embryonic development, the effect of this peptide on microbiota development was investigated. Embryos have long been considered sterile, but this paradigm is challenged by putative reports of bacteria in amniotic fluid and fetal membranes [42]. In embryonated chicken eggs, bacteria were also detected by culture-based methods [43]. However, in the present study using a sequencing-based approach, no detectable microbiota was found in 18-day old chicken embryos.

Large differences in microbiota composition were observed between two separate experiments and clustering of samples also correlated to housing of the chickens, indicating that microbiota was more strongly influenced by environmental factors than by CATH-2 treatment. The so-called ‘cage effect’ is a well-known confounding factor in microbiota studies in mice [44], one study estimated cage to contribute for 31% to the variance in murine microbiota composition [45]. Like mice, chickens are coprophagic animals; thus, a strongly shared microbiota within one cage is to be expected. In addition, large differences in microbiota composition were previously described between three repeated chicken trials [46]. Commercial chickens hatched in hatcheries are not colonized by microbiota derived from their mothers like in mammals but pick up their initial flora from the environment or handlers, leading to highly variable microbiota development. These results emphasize the importance of repeated trials to show the real effect of an examined treatment on microbiota composition.

The HDPs α -defensin 5 and LL-37 were previously shown to have an effect on microbiota composition in rodents [47,48]. In our study, D-CATH-2 was able to reproducibly affect abundance of a number of bacterial families and genera in both the ileum and cecum. Diversity of the microbiota was not affected by D-CATH-2 in contrast to regular antibiotics which decrease overall diversity of chicken microbiota and also reduce *Lactobacillus* and promote Clostridia species [49]. The most clear-cut result of D-CATH-2 administration was the reduction of *Escherichia/Shigella* in both ileum and cecum. *Escherichia/Shigella* are potential pathogens and abundance of this genus was found to correlate negatively with growth and fat digestibility in broiler chickens [50]. High numbers of *E. coli* in mouse microbiota were also shown to correlate to higher susceptibility to colonization by *Salmonella* [51]. Finally, *Escherichia/Shigella* was implicated in the pathogenesis of inflammatory bowel disease in both mouse models and human studies [52–54]. Reduction of *Escherichia/Shigella* might therefore be considered a positive effect of D-CATH-2 administration. Interestingly, both chickens administered yeast overexpressing the porcine cathelicidin PMAP-36 and piglets with diarrhea treated with a snake cathelicidin showed reduced *E. coli* counts in respectively cecal content and feces

[38,55], indicating that effects on this genus could be a more general HDP effect. In addition to the effect on *Escherichia/Shigella*, D-CATH-2 treatment also reproducibly reduced abundance of Ruminococcaceae and the genus *Butyricoccus* belonging to this Family. *Butyricoccus* and Ruminococcaceae in general are butyrate producing bacteria and considered beneficial members of the microbiota. Reduction of Ruminococcaceae abundance is correlated with diarrhea in both humans and dogs [56,57]. D-CATH-2 administration thus seems to have both beneficial and possibly unwanted influences on the intestinal microbiota. Additional work is needed to clarify these effects and the possible functional consequences on chicken performance and immune function.

In conclusion, *in ovo* administration of CATH-2 analogs showed little effect on the immune status of naïve chickens 7 days posthatch, suggesting that an infective stimulus is needed for the effect of the peptides to become apparent. However, D-CATH-2 treatment did affect several bacterial taxa, indicating that modulation of the gut microbiota might be one of the *in vivo* mechanisms of D-CATH-2.

Supporting information

S1 Fig. Chicken bodyweight over the course of the experiment. Weight curve from combined data from the three repeated experiments ($n = 6-11$ chickens/group in each experiment); depicted are mean \pm s.d. Data of independent experiments were analyzed by an unpaired *t*-test, overall data were analyzed using a General Linear Model.

(TIF)

S2 Fig. Expression of MHC-II and CD40 on KUL01 positive peripheral blood mononuclear phagocytes derived from Exp II. (a) MHC-II, (b) CD40. Depicted are mean fluorescence \pm s.d., $n = 6$ /group. Data were analyzed by an unpaired *t*-test.

(TIF)

S3 Fig. Leukocyte populations in cecal tonsils and spleen from Exp II. (a) cecal tonsils, (b) spleen. Total leukocytes (CD45), mononuclear phagocytes (KUL01), T-cells (CD3), B-cells (Bu-1), thrombocytes (CD41/CD61). Depicted are mean percentages of cells \pm s.d., $n = 6-7$ /group, n.d. = non-detectable. Data were analyzed by an unpaired *t*-test.

(TIF)

S4 Fig. Oxidative burst of PBMCs stimulated with PMA. Oxidative burst (stimulated with 1 μ g/ml PMA) measured by conversion of DCFH-DA to fluorescent DCF. Increase in fluorescence in 3 hours of incubation. Data from three repeated experiments. Depicted are mean \pm s.d., $n = 5-8$ /group. Data from independent experiments were analyzed by an unpaired *t*-test, combined data were analyzed by a General Linear Model.

(TIF)

S5 Fig. Intestinal architecture and goblet cell parameters in ileum and jejunum of 7 day old chicks. Data from three repeated experiments. (a)-(b) Villus/crypt ratio, (c)-(d) Goblet cell numbers per villus, (e)-(f) Goblet cell size. Depicted are mean \pm s.d., $n = 6-7$ /group. Data were analyzed by an unpaired *t*-test, combined data were analyzed using a General Linear Model.

(TIF)

S6 Fig. PCA plots of the bacterial communities in individual ileal samples. (a) ileal microbiota in Exp I, (b) ileal microbiota in Exp III, (c) combined ileal microbiota data from Exp I and III.

(TIF)

S7 Fig. Measures of alpha diversity of ileal and cecal microbiota. (a) Richness as defined by number of OTUs, (b) Shannon diversity index which takes into account both relative abundance and evenness of species in a sample. * = $p < 0.05$, ** = $p < 0.01$. Data were analyzed by unpaired *t*-test or Mann-Whitney *U* test in the case of non-normally distributed data. (TIF)

S1 Table. Results of microarray analysis. Differentially expressed genes between PBMCs from chickens treated with D-CATH-2 and control. Data were analyzed by Linear Model for Microarray Analysis (LIMMA) with Benjamini-Hochberg FDR correction. (PDF)

Acknowledgments

We would like to thank Marius Dwars of the Department of Farm Animal Health, Faculty of Veterinary Medicine, Utrecht University, for his help with the chicken sections. We are grateful to Marian Groot Koerkamp of the UMC Utrecht Microarray Facility for her help in analyzing the microarray data.

Author Contributions

Conceptualization: Tryntsje Cuperus, Albert van Dijk, Henk P. Haagsman.

Data curation: Aldert L. Zomer.

Formal analysis: Tryntsje Cuperus, Marina D. Kraaij, Aldert L. Zomer, Albert van Dijk, Henk P. Haagsman.

Funding acquisition: Henk P. Haagsman.

Investigation: Tryntsje Cuperus, Marina D. Kraaij, Aldert L. Zomer, Albert van Dijk.

Methodology: Tryntsje Cuperus, Marina D. Kraaij, Aldert L. Zomer, Henk P. Haagsman.

Project administration: Henk P. Haagsman.

Resources: Henk P. Haagsman.

Supervision: Henk P. Haagsman.

Writing – original draft: Tryntsje Cuperus.

Writing – review & editing: Albert van Dijk, Henk P. Haagsman.

References

1. Steinstraesser L, Kraneburg U, Jacobsen F, Al-Benna S. Host defense peptides and their antimicrobial-immunomodulatory duality. *Immunobiology* 2011 Mar; 216(3):322–333. <https://doi.org/10.1016/j.imbio.2010.07.003> PMID: 20828865
2. Mansour SC, Pena OM, Hancock RE. Host defense peptides: front-line immunomodulators. *Trends Immunol* 2014 Sep; 35(9):443–450. <https://doi.org/10.1016/j.it.2014.07.004> PMID: 25113635
3. Hancock RE, Sahl HG. Antimicrobial and host-defense peptides as new anti-infective therapeutic strategies. *Nat Biotechnol* 2006 Dec; 24(12):1551–1557. <https://doi.org/10.1038/nbt1267> PMID: 17160061
4. Cheng G, Hao H, Xie S, Wang X, Dai M, Huang L, et al. Antibiotic alternatives: the substitution of antibiotics in animal husbandry? *Front Microbiol* 2014 May 13; 5:217. <https://doi.org/10.3389/fmicb.2014.00217> PMID: 24860564
5. Baranska-Rybak W, Sonesson A, Nowicki R, Schmidtchen A. Glycosaminoglycans inhibit the antibacterial activity of LL-37 in biological fluids. *J Antimicrob Chemother* 2006 Feb; 57(2):260–265. <https://doi.org/10.1093/jac/dki460> PMID: 16387752

6. Wang Y, Agerberth B, Lothgren A, Almstedt A, Johansson J. Apolipoprotein A-I binds and inhibits the human antibacterial/cytotoxic peptide LL-37. *J Biol Chem* 1998 Dec 11; 273(50):33115–33118. PMID: [9837875](https://pubmed.ncbi.nlm.nih.gov/9837875/)
7. Kandasamy SK, Larson RG. Effect of salt on the interactions of antimicrobial peptides with zwitterionic lipid bilayers. *Biochim Biophys Acta* 2006 Sep; 1758(9):1274–1284. <https://doi.org/10.1016/j.bbamer.2006.02.030> PMID: [16603122](https://pubmed.ncbi.nlm.nih.gov/16603122/)
8. Nijnik A, Madera L, Ma S, Waldbrook M, Elliott MR, Easton DM, et al. Synthetic cationic peptide IDR-1002 provides protection against bacterial infections through chemokine induction and enhanced leukocyte recruitment. *J Immunol* 2010 Mar 1; 184(5):2539–2550. <https://doi.org/10.4049/jimmunol.0901813> PMID: [20107187](https://pubmed.ncbi.nlm.nih.gov/20107187/)
9. Scott MG, Dullaghan E, Mookherjee N, Glavas N, Waldbrook M, Thompson A, et al. An anti-infective peptide that selectively modulates the innate immune response. *Nat Biotechnol* 2007 Apr; 25(4):465–472. <https://doi.org/10.1038/nbt1288> PMID: [17384586](https://pubmed.ncbi.nlm.nih.gov/17384586/)
10. Cuperus T, van Dijk A, Matthijs MG, Veldhuizen EJ, Haagsman HP. Protective effect of *in ovo* treatment with the chicken cathelicidin analog D-CATH-2 against avian pathogenic *E. coli*. *Sci Rep* 2016 May 27; 6:26622. <https://doi.org/10.1038/srep26622> PMID: [27229866](https://pubmed.ncbi.nlm.nih.gov/27229866/)
11. Coorens M, van Dijk A, Bikker F, Veldhuizen EJ, Haagsman HP. Importance of Endosomal Cathelicidin Degradation To Enhance DNA-Induced Chicken Macrophage Activation. *J Immunol* 2015 Oct 15; 195(8):3970–3977. <https://doi.org/10.4049/jimmunol.1501242> PMID: [26378074](https://pubmed.ncbi.nlm.nih.gov/26378074/)
12. van Dijk A, van Eldik M, Veldhuizen EJA, Tjeerdma-van Bokhoven JL, de Zoete MR, Bikker FJ, et al. Immunomodulatory and anti-inflammatory activities of chicken cathelicidin-2 derived peptides. *PLOS One* 2016; 11(2):e0147919. <https://doi.org/10.1371/journal.pone.0147919> PMID: [26848845](https://pubmed.ncbi.nlm.nih.gov/26848845/)
13. van Wageningen S, Kemmeren P, Lijnzaad P, Margaritis T, Benschop JJ, de Castro IJ, et al. Functional overlap and regulatory links shape genetic interactions between signaling pathways. *Cell* 2010 Dec 10; 143(6):991–1004. <https://doi.org/10.1016/j.cell.2010.11.021> PMID: [21145464](https://pubmed.ncbi.nlm.nih.gov/21145464/)
14. Yang YH, Dudoit S, Luu P, Lin DM, Peng V, Ngai J, et al. Normalization for cDNA microarray data: a robust composite method addressing single and multiple slide systematic variation. *Nucleic Acids Res* 2002 Feb 15; 30(4):e15. PMID: [11842121](https://pubmed.ncbi.nlm.nih.gov/11842121/)
15. Margaritis T, Lijnzaad P, van Leenen D, Bouwmeester D, Kemmeren P, van Hooff SR, et al. Adaptable gene-specific dye bias correction for two-channel DNA microarrays. *Mol Syst Biol* 2009; 5:266. <https://doi.org/10.1038/msb.2009.21> PMID: [19401678](https://pubmed.ncbi.nlm.nih.gov/19401678/)
16. Wu Z, Rothwell L, Young JR, Kaufman J, Butter C, Kaiser P. Generation and characterization of chicken bone marrow-derived dendritic cells. *Immunology* 2010 Jan; 129(1):133–145. <https://doi.org/10.1111/j.1365-2567.2009.03129.x> PMID: [19909375](https://pubmed.ncbi.nlm.nih.gov/19909375/)
17. Luna L. *AFIP Manual of Histological Staining Methods*. 3rd ed. New York: McGraw Hill Publications; 1968.
18. Biesbroek G, Sanders EA, Roeselers G, Wang X, Caspers MP, Trzcinski K, et al. Deep sequencing analyses of low density microbial communities: working at the boundary of accurate microbiota detection. *PLoS One* 2012; 7(3):e32942. <https://doi.org/10.1371/journal.pone.0032942> PMID: [22412957](https://pubmed.ncbi.nlm.nih.gov/22412957/)
19. Schloss PD, Westcott SL, Ryabin T, Hall JR, Hartmann M, Hollister EB, et al. Introducing mothur: open-source, platform-independent, community-supported software for describing and comparing microbial communities. *Appl Environ Microbiol* 2009 Dec; 75(23):7537–7541. <https://doi.org/10.1128/AEM.01541-09> PMID: [19801464](https://pubmed.ncbi.nlm.nih.gov/19801464/)
20. Cole JR, Chai B, Marsh TL, Farris RJ, Wang Q, Kulam SA, et al. The Ribosomal Database Project (RDP-II): previewing a new autoaligner that allows regular updates and the new prokaryotic taxonomy. *Nucleic Acids Res* 2003 Jan 1; 31(1):442–443. PMID: [12520046](https://pubmed.ncbi.nlm.nih.gov/12520046/)
21. Brown KL, Poon GF, Birkenhead D, Pena OM, Falsafi R, Dahlgren C, et al. Host defense peptide LL-37 selectively reduces proinflammatory macrophage responses. *J Immunol* 2011 May 1; 186(9):5497–5505. <https://doi.org/10.4049/jimmunol.1002508> PMID: [21441450](https://pubmed.ncbi.nlm.nih.gov/21441450/)
22. Murakami T, Obata T, Kuwahara-Arai K, Tamura H, Hiramatsu K, Nagaoka I. Antimicrobial cathelicidin polypeptide CAP11 suppresses the production and release of septic mediators in D-galactosamine-sensitized endotoxin shock mice. *Int Immunol* 2009 Aug; 21(8):905–912. <https://doi.org/10.1093/intimm/dxp057> PMID: [19556302](https://pubmed.ncbi.nlm.nih.gov/19556302/)
23. Hou M, Zhang N, Yang J, Meng X, Yang R, Li J, et al. Antimicrobial peptide LL-37 and IDR-1 ameliorate MRSA pneumonia *in vivo*. *Cell Physiol Biochem* 2013; 32(3):614–623. <https://doi.org/10.1159/000354465> PMID: [24021961](https://pubmed.ncbi.nlm.nih.gov/24021961/)
24. Nizet V, Ohtake T, Lauth X, Trowbridge J, Rudisill J, Dorschner RA, et al. Innate antimicrobial peptide protects the skin from invasive bacterial infection. *Nature* 2001 Nov 22; 414(6862):454–457. <https://doi.org/10.1038/35106587> PMID: [11719807](https://pubmed.ncbi.nlm.nih.gov/11719807/)

25. Kovach MA, Ballinger MN, Newstead MW, Zeng X, Bhan U, Yu FS, et al. Cathelicidin-related antimicrobial peptide is required for effective lung mucosal immunity in Gram-negative bacterial pneumonia. *J Immunol* 2012 Jul 1; 189(1):304–311. <https://doi.org/10.4049/jimmunol.1103196> PMID: 22634613
26. Kogut MH, Genovese KJ, He H, Li MA, Jiang YW. The effects of the BT/TAMUS 2032 cationic peptides on innate immunity and susceptibility of young chickens to extraintestinal *Salmonella enterica* serovar Enteritidis infection. *Int Immunopharmacol* 2007 Jul; 7(7):912–919. <https://doi.org/10.1016/j.intimp.2007.02.011> PMID: 17499193
27. Kogut MH, He H, Genovese KJ, Jiang YW. Feeding the BT cationic peptides to chickens at hatch reduces cecal colonization by *Salmonella enterica* serovar Enteritidis and primes innate immune cell functional activity. *Foodborne Pathog Dis* 2010 Jan; 7(1):23–30. <https://doi.org/10.1089/fpd.2009.0346> PMID: 19735207
28. Saeed S, Quintin J, Kerstens HH, Rao NA, Aghajani-refah A, Matarese F, et al. Epigenetic programming of monocyte-to-macrophage differentiation and trained innate immunity. *Science* 2014 Sep 26; 345(6204):1251086. <https://doi.org/10.1126/science.1251086> PMID: 25258085
29. Quintin J, Saeed S, Martens JH, Giamarellos-Bourboulis EJ, Iffrim DC, Logie C, et al. *Candida albicans* infection affords protection against reinfection via functional reprogramming of monocytes. *Cell Host Microbe* 2012 Aug 16; 12(2):223–232. <https://doi.org/10.1016/j.chom.2012.06.006> PMID: 22901542
30. Uni Z, Noy Y, Sklan D. Posthatch changes in morphology and function of the small intestines in heavy- and light-strain chicks. *Poult Sci* 1995 Oct; 74(10):1622–1629. <https://doi.org/10.3382/ps.0741622> PMID: 8559726
31. Uni Z, Tako E, Gal-Garber O, Sklan D. Morphological, molecular, and functional changes in the chicken small intestine of the late-term embryo. *Poult Sci* 2003 Nov; 82(11):1747–1754. <https://doi.org/10.1093/ps/82.11.1747> PMID: 14653469
32. Uni Z, Smirnov A, Sklan D. Pre- and posthatch development of goblet cells in the broiler small intestine: effect of delayed access to feed. *Poult Sci* 2003 Feb; 82(2):320–327. <https://doi.org/10.1093/ps/82.2.320> PMID: 12619811
33. Fasina YO, Hoerr FJ, McKee SR, Conner DE. Influence of *Salmonella enterica* serovar Typhimurium infection on intestinal goblet cells and villous morphology in broiler chicks. *Avian Dis* 2010 Jun; 54(2):841–847. <https://doi.org/10.1637/9055-090809-Reg.1> PMID: 20608528
34. Cheled-Shoval SL, Amit-Romach E, Barbakov M, Uni Z. The effect of *in ovo* administration of mannan oligosaccharide on small intestine development during the pre- and posthatch periods in chickens. *Poult Sci* 2011 Oct; 90(10):2301–2310. <https://doi.org/10.3382/ps.2011-01488> PMID: 21934014
35. Czerwinski J, Hojberg O, Smulikowska S, Engberg RM, Mieczkowska A. Effects of sodium butyrate and salinomycin upon intestinal microbiota, mucosal morphology and performance of broiler chickens. *Arch Anim Nutr* 2012 Apr; 66(2):102–116. PMID: 22641923
36. Baurhoo B, Ferket PR, Zhao X. Effects of diets containing different concentrations of mannanoligosaccharide or antibiotics on growth performance, intestinal development, cecal and litter microbial populations, and carcass parameters of broilers. *Poult Sci* 2009 Nov; 88(11):2262–2272. <https://doi.org/10.3382/ps.2008-00562> PMID: 19834074
37. Tai EK, Wong HP, Lam EK, Wu WK, Yu L, Koo MW, et al. Cathelicidin stimulates colonic mucus synthesis by up-regulating MUC1 and MUC2 expression through a mitogen-activated protein kinase pathway. *J Cell Biochem* 2008 May 1; 104(1):251–258. <https://doi.org/10.1002/jcb.21615> PMID: 18059019
38. Yi H, Zhang L, Gan Z, Xiong H, Yu C, Du H, et al. High therapeutic efficacy of Cathelicidin-WA against postweaning diarrhea via inhibiting inflammation and enhancing epithelial barrier in the intestine. *Sci Rep* 2016 May 16; 6:25679. <https://doi.org/10.1038/srep25679> PMID: 27181680
39. Tomkovich S, Jobin C. Microbiota and host immune responses: a love-hate relationship. *Immunology* 2016 Jan; 147(1):1–10. <https://doi.org/10.1111/imm.12538> PMID: 26439191
40. Kabat AM, Srinivasan N, Maloy KJ. Modulation of immune development and function by intestinal microbiota. *Trends Immunol* 2014 Nov; 35(11):507–517. <https://doi.org/10.1016/j.it.2014.07.010> PMID: 25172617
41. Tamburini S, Shen N, Wu HC, Clemente JC. The microbiome in early life: implications for health outcomes. *Nat Med* 2016 Jul 7; 22(7):713–722. <https://doi.org/10.1038/nm.4142> PMID: 27387886
42. Funkhouser LJ, Bordenstein SR. Mom knows best: the universality of maternal microbial transmission. *PLoS Biol* 2013; 11(8):e1001631. <https://doi.org/10.1371/journal.pbio.1001631> PMID: 23976878
43. Kizerwetter-Swida M, Binek M. Bacterial microflora of the chicken embryos and newly hatched chicken. *Journal of Animal and Feed Sciences* 2008 2008; 17(2):224–232.
44. McCafferty J, Muhlbauer M, Gharaibeh RZ, Arthur JC, Perez-Chanona E, Sha W, et al. Stochastic changes over time and not founder effects drive cage effects in microbial community assembly in a

- mouse model. *ISME J* 2013 Nov; 7(11):2116–2125. <https://doi.org/10.1038/ismej.2013.106> PMID: 23823492
45. Hildebrand F, Nguyen TL, Brinkman B, Yunta RG, Cauwe B, Vandenabeele P, et al. Inflammation-associated enterotypes, host genotype, cage and inter-individual effects drive gut microbiota variation in common laboratory mice. *Genome Biol* 2013 Jan 24; 14(1):R4-2013-14-1-r4. <https://doi.org/10.1186/gb-2013-14-1-r4> PMID: 23347395
 46. Stanley D, Geier MS, Hughes RJ, Denman SE, Moore RJ. Highly variable microbiota development in the chicken gastrointestinal tract. *PLoS One* 2013 Dec 31; 8(12):e84290. <https://doi.org/10.1371/journal.pone.0084290> PMID: 24391931
 47. Pound LD, Patrick C, Eberhard CE, Mottawea W, Wang GS, Abujamel T, et al. Cathelicidin Antimicrobial Peptide: A Novel Regulator of Islet Function, Islet Regeneration, and Selected Gut Bacteria. *Diabetes* 2015 Dec; 64(12):4135–4147. <https://doi.org/10.2337/db15-0788> PMID: 26370175
 48. Salzman NH, Hung K, Haribhai D, Chu H, Karlsson-Sjoberg J, Amir E, et al. Enteric defensins are essential regulators of intestinal microbial ecology. *Nat Immunol* 2010 Jan; 11(1):76–83. <https://doi.org/10.1038/ni.1825> PMID: 19855381
 49. Lu J, Hofacre C, Smith F, Lee MD. Effects of feed additives on the development on the ileal bacterial community of the broiler chicken. *Animal* 2008 May; 2(5):669–676. <https://doi.org/10.1017/S1751731108001894> PMID: 22443592
 50. Rubio LA, Peinado MJ, Ruiz R, Suarez-Pereira E, Ortiz Mellet C, Garcia Fernandez JM. Correlations between changes in intestinal microbiota composition and performance parameters in broiler chickens. *J Anim Physiol Anim Nutr (Berl)* 2015 Jun; 99(3):418–423.
 51. Stecher B, Chaffron S, Kappeli R, Hapfelmeier S, Friedrich S, Weber TC, et al. Like will to like: abundances of closely related species can predict susceptibility to intestinal colonization by pathogenic and commensal bacteria. *PLoS Pathog* 2010 Jan; 6(1):e1000711. <https://doi.org/10.1371/journal.ppat.1000711> PMID: 20062525
 52. Bassett SA, Young W, Barnett MP, Cookson AL, McNabb WC, Roy NC. Changes in composition of caecal microbiota associated with increased colon inflammation in interleukin-10 gene-deficient mice inoculated with *Enterococcus* species. *Nutrients* 2015 Mar 11; 7(3):1798–1816. <https://doi.org/10.3390/nu7031798> PMID: 25768951
 53. Chen L, Wang W, Zhou R, Ng SC, Li J, Huang M, et al. Characteristics of fecal and mucosa-associated microbiota in Chinese patients with inflammatory bowel disease. *Medicine (Baltimore)* 2014 Aug; 93(8):e51.
 54. Thorkildsen LT, Nwosu FC, Avershina E, Ricanek P, Perminow G, Brackmann S, et al. Dominant fecal microbiota in newly diagnosed untreated inflammatory bowel disease patients. *Gastroenterol Res Pract* 2013; 2013:636785. <https://doi.org/10.1155/2013/636785> PMID: 24348539
 55. Wang L, Zhang H, Jia Z, Ma Q, Dong N, Shan A. In vitro and in vivo activity of the dimer of PMAP-36 expressed in *Pichia pastoris*. *J Mol Microbiol Biotechnol* 2014; 24(4):234–240. <https://doi.org/10.1159/000365572> PMID: 25196715
 56. Guard BC, Barr JW, Reddivari L, Klemashevich C, Jayaraman A, Steiner JM, et al. Characterization of microbial dysbiosis and metabolomic changes in dogs with acute diarrhea. *PLoS One* 2015 May 22; 10(5):e0127259. <https://doi.org/10.1371/journal.pone.0127259> PMID: 26000959
 57. Schubert AM, Rogers MA, Ring C, Mogle J, Petrosino JP, Young VB, et al. Microbiome data distinguish patients with *Clostridium difficile* infection and non-*C. difficile*-associated diarrhea from healthy controls. *MBio* 2014 May 6; 5(3):e01021–14. <https://doi.org/10.1128/mBio.01021-14> PMID: 24803517